

# TEFC Induction Motors Thermal Models: A Parameter Sensitivity Analysis

A. Boglietti\*, A. Cavagnino\*, D.A. Staton #

Dip. Ingegneria Elettrica Industriale - Politecnico di Torino – C.so Duca degli Abruzzi, 24,  
10129 Torino - ITALY

# Motor Design Ltd, 1 Eaton Court, Tetchill, Ellesmere, Shropshire, UK

**Abstract** With the increasing pressures on electric motor manufactures to develop smaller and more efficient electric motors, there is a trend to carry out more thermal analysis in parallel with the traditional electromagnetic design. It has been found that attention to thermal design can be rewarded by major improvements in the overall performance. Thus, there is a requirement for accurate and reliable thermal analysis models that can be easily incorporated into motor design software. In the paper emphasis is given to thermal sensitivity analysis of Total Enclosed Fan Cooled (TEFC) induction motors. In particular, thermal parameters are modified and their effects on the temperature rise shown. The results are useful for identifying the most important thermal parameters and enables robust designs to be developed that are insensitive to manufacturing tolerances.

## I. INTRODUCTION

Thermal analysis software is typically based on either analytical lumped circuit or numerical models. In this paper we will use an analytical lumped circuit model as its calculation speed is most appropriate for the large number of calculations required when carrying out sensitivity analysis [1-3]. The main strength of numerical computational fluid dynamics (CFD) software is that it can be used to predict flow in complex regions such as around the end windings [2-4]. Numerical finite element analysis (FEA) software must use analytical/empirical based algorithms for convection boundaries, as used in lumped circuit analysis. Its only advantage is that it can model solid component conduction more accurately. Numerical analysis suffers from long model setup and computation times, especially as it is virtually impossible to reduce the problem to two dimensions. Data obtained using CFD can most usefully be used to improve the analytical algorithms used in the analytical software [2,3].

The circuit, shown in Fig.1, is a three dimensional representation of the main heat transfer paths within an induction motor. Thermal resistances for the conduction heat transfer paths are calculated from the dimensions and thermal conductivity of each component. Radiation is calculated using emissivity and view factor coefficients and component surface area. Convection thermal resistances (natural and forced) are calculated using proven

empirical correlations which are based on dimensional analysis [5]. More details of the model can be found in [3].

One useful feature of the thermal software used is the implementation of ActiveX technology that allows the design process to be fully automated. Matlab or Excel VBA scripts are written to vary parameters over a given range and to plot graphs of the variation in component temperatures. This is very useful when carrying out sensitivity analysis. ActiveX technology also has the advantage that the thermal software can be directly linked to other software packages such as electromagnetic design software. Powerful combined packages can be developed that account for the fact that the temperature rise depends on the losses and the losses depend on the temperature.

Thermal models have been developed for the five industrial induction motors shown in Fig.2 (rated power: 4 kW – 7.5 kW – 15 kW – 30 kW – 55 kW, 4 poles, 380 V, 50 Hz). All the motors are thermally monitored with PT100 sensors. Three sensors have been positioned on the end windings (one for each phase). Another sensor is inserted inside a stator slot and the last sensor has been included in a hole positioned in the stator core. This measurement setup allows us to measure winding and iron core temperatures during the tests. The housing temperature has been measured by means of a digital thermometer taking into account several positions on the housing surface.

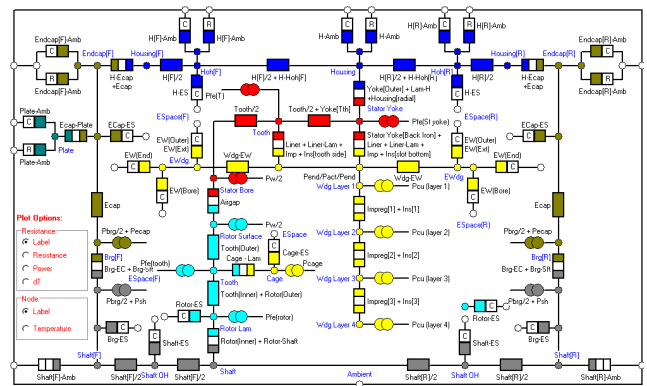


Fig.1: Lumped Circuit for an induction motor thermal model

The thermal models developed have been experimentally verified. The results obtained using the software's default parameters have been compared with solutions obtained using tuned parameters obtained through thermal tests (calibrated models). The analysis and the results reported in the paper can be used as general guidelines useful for obtaining accurate thermal models of TEFC induction motors. Two thermal test setups have been considered. One is based on a DC supply and the other on a variable frequency AC supply.



Fig.2: Induction Motors used in the analysis

## II. DC THERMAL TEST AND MODELS

In this test only stator copper loss exists. During the test the DC supply current is equal to 50÷70% of the rated current. The reduced current is required to avoid thermal damage due to zero cooling air speed. At thermal steady state, the adsorbed electrical power and the temperatures of the stator windings, stator core and external housing have been measured. Two thermal models have been taken into consideration. The first one (termed the “Complete DC thermal model”) includes radiation. The second one (termed the “Simplified DC thermal model”) the radiation has been neglected. The second model is based on the general assumption that the highest temperature on the motor frame is not high enough to give a significant amount of radiation heat transfer. Following the procedure described in [7], both the thermal models have been calibrated until the predicted temperatures equal the measured ones. For the Complete DC model the calibration has been done by modifying the following thermal parameters:

- $K_h$  coefficient used to multiply the natural convection heat natural transfer coefficient “h” as calculated by standard dimensionless analysis correlations [5].
- impregnation varnish thermal conductivity [W/m°C]
- housing surface radiation emissivity [pu]
- impregnation goodness. This is used to account for imperfections in the impregnation process. A value of 1 means a perfect impregnation without air bubbles while a factor of 0 means no impregnation (all air).
- interface gap between housing and stator lamination [mm].

The interface gap is due to microscopic imperfections in magnetic cores outer surface and the frames inner surface. This leads to limited points of contact at surface high spots with air voids in-between. Heat transfer through the touching spots and voids is essentially by conduction. The thermal contact resistance can be large as air has a low thermal conductivity. The five quantities listed above have been selected as key thermal coefficients on the basis of the analysis reported in [6]. It is noted that the impregnation goodness and impregnation varnish thermal conductivity are not independent of each other in terms of the motor thermal behavior. It is possible to get a calibrated model using a range of coupled values. As a consequence, in order to simplify the problems, two methods have been used in the sensitivity analysis.

### Method 1

The impregnation varnish thermal conductivity is set equal to a value reported in its material data sheet. The impregnation goodness is considered to be the variable parameter.

### Method 2

The impregnation goodness is set equal to 1 (perfect impregnation without air bubbles). The varnish thermal conductivity is considered to be the variable parameter.

In practice it is a matter of preference and available data which method is used. In some cases accurate thermal conductivity data for the varnish may not be available and the designer has to make an estimate. The correct impregnation goodness factor is strongly influenced by the impregnation process whose quality may not be a constant quantity. If accurate varnish data is available then the impregnation goodness factor gives a good indication of the quality of the process used.

Tables I to IV show the parameters required to calibrate the four DC thermal test models discussed (all 5 motors).

TABLE I  
Value of the calibrated model parameter for the five motors  
(Complete DC thermal model – Method 1)

	4. kW	7.5 kW	15 kW	30 kW	55 kW
$K_h$	0.95	0.87	0.95	1.00	1.35
impregnation goodness	0.4	0.4	0.3	0.45	0.5
interface gap [mm]	0.04	0.08	0.07	0.01	0.02

TABLE II  
Value of the calibrated model parameter for the five motors  
(Complete DC thermal model - Method 2)

	4. kW	7.5 kW	15 kW	30 kW	55 kW
$K_h$	0.95	0.87	0.95	1.00	1.35
impregnation varnish thermal conductivity [W/m/C]	0.07	0.07	0.07	0.075	0.08
interface gap [mm]	0.04	0.08	0.07	0.01	0.02

TABLE III  
Value of the calibrated model parameter for the five motors  
(Simplified DC thermal model - Method 1)

	4. kW	7.5 kW	15 kW	30 kW	55 kW
$K_h$	1.62	1.47	1.62	1.60	1.95
impregnation goodness	0.4	0.4	0.3	0.45	0.5
interface gap [mm]	0.04	0.08	0.07	0.01	0.02

TABLE IV  
Value of the calibrated model parameter for the five motors  
(Simplified DC thermal model- Method 2)

	4. kW	7.5 kW	15 kW	30 kW	55 kW
$K_h$	1.62	1.47	1.62	1.60	1.95
impregnation varnish thermal conductivity [W/m/C]	0.07	0.07	0.07	0.075	0.08
interface gap [mm]	0.04	0.08	0.07	0.01	0.02

In the complete DC thermal model an housing emissivity value of 0.8 has been used. A value of 0.8-0.95 is typical of painted components [3]. In the simplified DC thermal model the housing emissivity is set equal to 0. In Method 1 the varnish datasheet thermal conductivity of 0.13W/m/C is used. In Method 2 an impregnation goodness of 1 has been used. Comparing data in Tables I to IV it is evident that neglecting the radiation leads to a significant increase in  $K_h$ . This shows that radiation can give a significant component of cooling, especially when the cooling is by natural convection as is the case with zero fan speed. With unity impregnation goodness an equivalent impregnation varnish thermal conductivity of approximately 55% of the

datasheet value is necessary. This value gives a relatively good match with the average impregnation goodness factor of 0.45 for the five motor models that use the datasheet value of varnish thermal conductivity.

Sensitivity analysis results given in Tables V and VI relate to the winding temperatures rather than housing and lamination temperatures. The winding temperature was chosen as it is a critical quantity for assessing the motor life. The average winding temperature is quoted rather than the winding hotspot. The percentage variation in parameter values given in Tables V to VI are with reference to the calibrated model values reported in Tables I to IV.

TABLE V Winding average temperature variation in %  
Five motors (Complete DC thermal model)

	Thermal parameter Modification in [%]	Complete DC model Winding temperatures variation in %				
		4 kW	7.5 kW	15 kW	30 kW	55 kW
<b>Emissivity</b>	-80	15.42	17.0	13.89	14.36	9.57
<b>Radiation</b>	25	-3.39	-3.7	-3.10	-3.20	-2.26
<b>Impregnation goodness</b>	-80	5.06	4.1	3.70	8.26	7.09
	100	-2.35	-1.9	-1.94	-3.66	-2.97
<b>K<sub>h</sub></b>	-50	16.02	17.0	14.54	17.30	18.47
	50	-8.91	-9.8	-8.09	-9.47	-10.68
<b>Gap housing-iron</b>	-80	-2.35	-4.5	-2.67	-0.51	-0.92
	100	2.83	5.4	3.23	0.63	1.16
<b>Impregnation varnish conductivity</b>	-80	23.72	20.0	19.49	34.32	27.22
	100	-3.34	-2.7	-2.67	-5.05	-4.00

TABLE VI Winding average temperature variation in %  
Five motors (Simplified DC thermal model)

	Thermal parameter Modification in [%]	Simplified DC model Winding temperatures variation in %				
		4 kW	7.5 kW	15 kW	30 kW	55 kW
<b>K<sub>h</sub></b>	-50	33.73	37.6	29.27	34.13	30.91
	50	-13.04	-14.1	-11.25	-14.64	-13.16
<b>Gap housing-iron</b>	-80	-2.36	-4.5	-2.70	-0.51	-0.94
	100	2.86	5.4	3.26	0.63	1.18
<b>Impregn. Varnish Conductivity</b>	-80	23.79	20.0	19.59	34.53	13.40
	100	-3.36	-2.7	-2.68	-5.09	-4.55

The following observations are made with regard to results shown in Tables V for the Complete DC Model:

- The winding temperature is most sensitive to the housing natural convection heat transfer coefficient “h”. This is the case for all five motors. A reduction of 50% leads to a 15÷18% increase in winding temperature. An increase of 50% corresponds to a winding temperature reduction of about 10%. The problem is that it is very difficult to incorporate design features that increase natural convection and do not reduce forced convection when the fan is operating, i.e. radial fins are usually used to increase natural convection but degrade shaft fan forced convection.
- The winding temperature is quite sensitive to radiation emissivity. An 80% reduction corresponds to a winding temperature increase of 14÷17%. On the contrary, 25% increase (maximum emissivity of 1) results in a 3% reduction in winding temperature. This highlights how important radiation can be when the cooling is by natural convection.
- With a constant value of the impregnation varnish conductivity (Method 1), the Impregnation Goodness is the third most important parameter. An 80% reduction gives a 4÷8% increase in winding temperature. A 100% increase gives a 2÷3% reduction in winding temperature. With a constant value of the impregnation goodness equal to 1 (Method 2), the model shows a higher sensitivity with respect to the impregnation varnish conductivity variation. A reduction of 60÷65% gives a 4÷7% increase in winding temperature. Larger reductions up to 80% lead to very rapid winding temperature increases up to 20÷34%. A 100% increase in thermal conductivity gives a 3÷5% drop in winding temperature.
- The winding temperature is not so sensitive to the interface gap. No more than a variation of ±5% in temperature is shown with an interface gap variation of ±80%. This is mainly due to the fact that the motors are not heavily loaded. In heavily loaded motors even a small thermal contact resistance can give a significant temperature drop.

The following observations are made with regard to results shown in Tables V for the Simplified DC Model:

- The winding temperature is most sensitive to the  $K_h$  coefficient (as in the complete model). A reduction of 50% gives a 35% increase in winding temperature. On the contrary an increase of 50% gives an 11÷15% decrease in winding temperature. The percentage changes in temperatures are larger than for the complete model again showing the significance of radiation, i.e. the radiation is included in the artificial increase in the  $K_h$  coefficient
- The impregnation varnish conductivity is quite important. With an impregnation goodness equal to 1 (Method 2), a 80% reduction in impregnation varnish conductivity leads to a 13÷35% increase in winding temperature. An increase of 100% corresponds to a winding temperature reduction of no more than 5%
- The model sensitivity to the interface gap is very small. In fact only a variation of  $\pm 5\%$  on the winding temperature has been found for an interface gap variation of  $-80\%$  and  $+100\%$ .

Fig. 3 gives a graphical example of sensitivity analysis results. In this case it shows the sensitivity analysis results on the winding temperature for the 55 kW motor.

It is evident that the thermal performance is more sensitive to some parameters than others. These results are useful to formulate trends and help check that expected manufacturing tolerances do not lead to unexpected results and incorrect thermal designs.

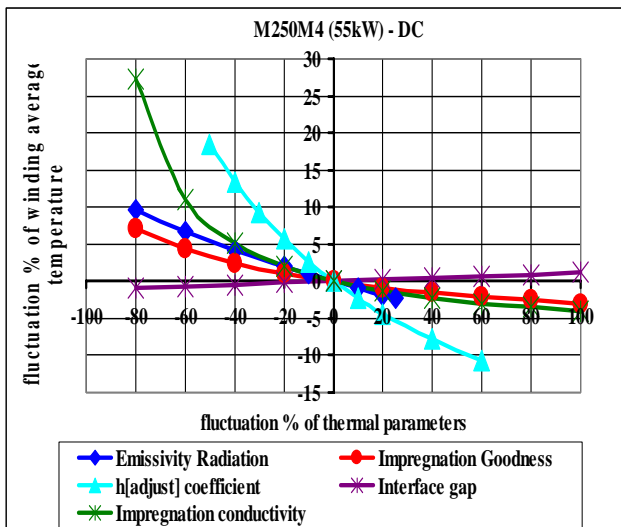


Fig. 3: DC model sensitivity analysis (55kW)

### III: VARIABLE FREQUENCY AC THERMAL TEST/MODELS

Thermal models for motors operating from PWM variable frequency (10 to 50 Hz) supplies have been compared with steady state thermal tests. Absorbed electrical power, mechanical power and the temperatures of the stator windings, stator core and external housing have been measured. In addition, the cooling air speed flowing in the open fin channels on the outside of the housing has been measured by means of a digital anemometer. The air speed variation along the channels (due to air leakage) and around the housing periphery has also been measured. The air speed has been confirmed to be the most critical quantity for an accurate thermal model [6,7]. As in the DC analysis, two models have been used for the AC thermal model sensitivity evaluation. Both AC thermal models use the same input parameters as those found using the corresponding calibrated DC model. The only parameter that needs further calibration is the air from the fan. The first model (termed the “Complete AC model”) uses a complex representation of the forced convection heat transfer coefficient “h” on the different axial surfaces of the motor frame, i.e. active and overhanging sections of the housing. In particular, the following parameters are taken into account:

- $h_a$  heat transfer coefficient of the housing active section (see Fig. 4)
- $h_f$  heat transfer coefficient of the housing front section (see Fig. 4)
- $h_r$  heat transfer coefficient of the housing rear section (see Fig. 4)
- Average value of the measured air speed at fan cowl output section.

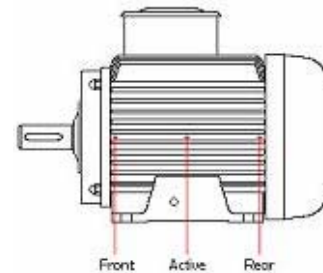


Fig. 4 : External motor frame reference.

The calibration procedure is as follows. Firstly, the measured average air speed from the fan cowling is input into the model (rear position in Fig. 4). This is considered as a reference values for which many motor manufactures have curves showing typical velocity (or more often volume flow rate) against shaft speed and motor (fan)

diameter. As expected, the air speed is maximum at the cowling outlet and reduces along the axial length of the motor due to leakage. The software uses leakage factors to define the magnitude of this air speed reduction along the axial length. We have varied these factors until the predicted temperatures are within  $\pm 5^\circ\text{C}$  of the measured values. The second model (termed the ‘‘Simplified AC model’’) is based on the calibrated simplified dc model where the housing radiation has been neglected. A constant cooling air speed has been considered over the full axial length of the motor external frame. The model calibration has been done by changing the value of this air speed until

the predicted temperatures are within  $\pm 5^\circ\text{C}$  of measured ones. In this simplified case the air speed is a theoretical value of the average air speed on the total external frame surface. Starting from the two calibrated models, the sensitivity analysis has been done on the 4 kW and 55 kW motors. Load tests have been performed at several frequencies. It is noted that the 55 kW motor has not been tested at 50 Hz due to test bench power limitations. The torque must be de-rated at lower frequencies due to the reduced cooling effects when the motor is rotating at lower speeds. More information on the tests performed can be found in [7].

TABLE VII  
Winding average temperature variation in %  
(55 kW motor - Complete AC thermal model)

	Thermal parameter Variation [%]	Complete AC thermal model 55 kW motor				
		Winding temperatures variation [%]				
		10 Hz	15 Hz	20 Hz	30 Hz	40 Hz
Air speed at the fan cowl output	-50	21.62	22.8	22.13	20.75	19.69
	50	-10.94	-10.2	-9.42	-8.58	-8.15
$h_f$ Housing [Front section]	-50	1.72	1.9	1.96	2.07	2.11
	50	-1.72	-1.6	-1.59	-1.60	-1.56
$h_a$ Housing [Active section]	-50	16.19	17.5	17.37	16.43	15.75
	50	-9.99	-9.4	-8.76	-7.97	-7.51
$h_r$ Housing [Rear section]	-50	3.96	3.7	3.45	3.19	3.02
	50	-2.76	-2.4	-2.15	-1.88	-1.83

TABLE VIII  
Winding average temperature variation in %  
(4 kW motor - Complete AC thermal model)

	Thermal parameter Variation [%]	Complete AC thermal model 4 kW motor					
		Winding temperatures variation [%]					
		10 Hz	15 Hz	20 Hz	30 Hz	40 Hz	50 Hz
Air speed at the fan cowl output	-50	15.86	20.0	20.97	20.84	20.71	20.40
	50	-10.03	-10.3	-9.99	-9.28	-8.96	-8.70
$h_f$ Housing [Front section]	-50	1.21	2.0	1.93	1.97	2.09	2.15
	50	-1.68	-2.0	-1.90	-1.81	-1.87	-1.88
$h_a$ Housing [Active section]	-50	8.68	11.6	12.86	12.69	12.47	12.16
	50	-7.46	-8.1	-8.23	-7.70	-7.44	-7.17
$h$ [adjust] Housing[Rear]	-50	5.78	5.9	5.47	5.38	5.14	5.17
	50	-4.85	-4.5	-4.10	-3.82	-3.62	-3.55
$h_r$ Housing [Rear section]	-50	7.74	10.0	10.88	10.68	10.43	10.12
	50	-6.16	-6.7	-6.80	-6.35	-6.14	-5.91

TABLE IX  
Winding average temperature variation in %  
(55 kW motor - Simplified AC thermal model)

	Thermal parameter Variation [%]	Complete AC thermal model 55 kW motor				
		Winding temperatures variation [%]				
		10 Hz	15 Hz	20 Hz	30 Hz	40 Hz
Average air speed on the housing surface	-50	24.77	24.62	23.71	21.69	20.32
	50	-10.98	10.16	-9.58	-8.62	-8.82

TABLE X  
Winding average temperature variation in %  
(4 kW motor - Simplified AC thermal model)

	Thermal parameter Variation [%]	Complete AC thermal model 4 kW motor					
		Winding temperatures variation [%]					
		10 Hz	15 Hz	20 Hz	30 Hz	40 Hz	50 Hz
Average air speed on the housing surface	-50	20.91	24.9	25.47	25.41	24.71	23.9
	50	-12.13	-11.63	-11.16	-10.47	-9.88	-9.40

The following observations are made with regard to results shown in Tables VII to X:

Complete AC thermal model: Tables VII and VIII

- The winding temperature is more sensitive to the air speed at the fan cowl output for all the supply frequencies. In particular a 50% reduction leads to a winding temperature increases of 20÷23%. On the contrary an increase of 50% leads to a winding temperature reduction of about 8÷11%.
- The heat transfer coefficient  $h_a$  is a sensitive parameter. A reduction of 50% gives a winding temperature increases of 16÷17%. An increase of 50% corresponds to a winding temperature reduction of about 8÷10%. The design is more sensitive to active heat transfer than overhang heat transfer as it forms a larger proportion of the housing cooling surface and is closer to the heat generation sources.
- The winding temperature does not show consistent sensitivity to the other parameters.

Simplified AC thermal model: Tables IX and X

- In the simplified thermal model, just an average cooling air speed is considered and obviously the winding temperature is very sensitive to this quantity. A variation of -50% leads to a temperature increase of up to 34%. Lower sensitivity is related to an air speed increase.

In order to get a reasonable prediction of the motor temperatures, both models require a correct evaluation of

the actual cooling air speed. Its measurement is not a simple task because there is a large air speed variation over housing surface. In fact in TEFC machines some of the fin channels on the outside of the machine are blocked by bolt lugs and terminal boxes. Another deficiency of TEFC machines is that the air leaks out of the open channels causing the local air velocity to be lower at the drive end than at the non-drive end. The prediction of the actual reduction in velocity is a complex function of many factors including the fan, fin and cowling design and rotational speed. In order to visualize the air speed distribution, accurate measurements in each fin channel on the motor housing have been performed using a digital anemometer. As an example, the measured distribution of air speed in the housing rear position is shown in Fig 6. The fin numeration used for the air speed measurements is given in Fig. 7. The effects of obstructions such as the fan cowl supports are clearly shown as speed dips. Fig.8 shows the air speed distribution along the axial direction for several of the fin channels. The leakage from the fins channels giving reduced velocity at the drive end is clearly seen.

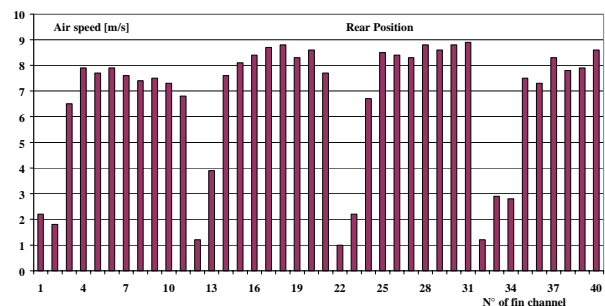


Fig.6: Air speed distribution around the housing rear position

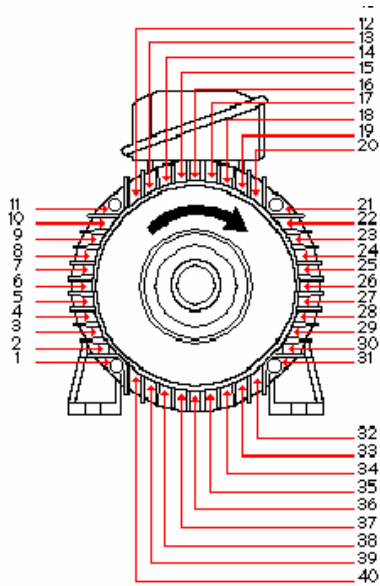


Fig.7: Fin channel numeration

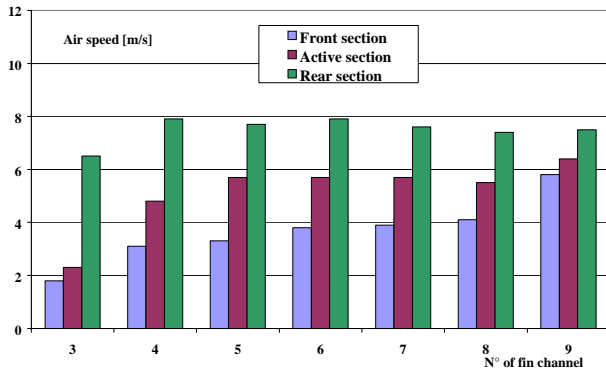


Fig.8: Air speed distribution in the axial direction in different fin channels

### III. GENERAL CONSIDERATIONS ON THE ANALYZED PROBLEMS

The problems discussed in the paper illustrate the complex nature of thermal analysis of TEFC motors and show how models can be calibrated using certain key parameters. Sensitivity analysis plays a fundamental role in being able to make judgments of the motor models accuracy. The authors make the following recommendations for developing accurate models:

- It is useful to use a DC test to calibrate the majority of the model calibration parameters. This removes a significant variable in form of the air blown over the machine.
- Simplified models that neglect radiation and/or open channel air leakage are suggested for the early stages of the design process when there may be large gaps in knowledge of key thermal parameters.

- Radiation can be significant at low rotational speeds and should be included in the model. It only requires knowledge of the housing surface finish (natural, painted, etc), for which well known emissivity data is readily available [3]. Inclusion of radiation also simplifies the calculation of natural convection as we do not need to adjust proven correlations to account for deficiencies in the radiation calculation.
- The housing fin channel air speed is the most sensitive quantity for a TEFC induction motor thermal model. Just a superficial knowledge of the motors geometrical properties is not sufficient to account for complexities such as fin channel leakage and blockage. Usually some measurement is required to obtain an accurate model as such complex air flow phenomena are very complex. Empirical and/or CFD data is available to help set realistic values at the start of a design.

### IV. CONCLUSIONS

In the paper the problems associated with calibration of thermal models and in particular sensitivity analysis of key model parameters is discussed. Thermal tests and simulations have been performed on five TEFC motors. Sensitivity analysis allows us to identify the most important thermal design variables and to make judgments of how sensitive the design is to the variation of such variables. The identification of such information is important when developing robust designs that are insensitive to manufacturing tolerances. Also, the research has demonstrated a good method for setting up thermal models for TEFC induction motors.

### REFERENCES

- [1] P.Mellor, D.Roberts, D. Turner, "Lumped parameter thermal model for electrical machines of TEFC design", IEE Proceedings, Vol. 138, September 1991.
- [2] D. Staton, S.J. Pickering, D. Lampard: "Recent Advancement in the Thermal Design of Electric Motors", SMMA 2001 Fall Technical Con., Durham. North Carolina, 3-5 Oct. 2001
- [3] D. Staton, "Thermal analysis of electric motors and generators", Tutorial course IEEE IAS Annual Meeting 2001, Chicago, USA.
- [4] J. Muggleston, S.J. Pickering, D. Lampard: "Effect of Geometry Changes on the Flow and Heat Transfer in the End Region of a TEFC Induction Motor", 9<sup>th</sup> IEE Intl. Con. Electrical Machines & Drives, Canterbury, UK, Sept 99
- [5] F.P. Incropera, D.P. DeWitt: Introduction to Heat Transfer, Wiley, 1990.
- [6] D. Staton, A. Boglietti, A. Cavagnino, "Solving the More Difficult Aspects of Electric Motor Thermal Analysis", IEMDC 2003, 1-4 June 2003, Madison Wisconsin, USA.
- [7] A. Boglietti, A. Cavagnino, D. Staton "Thermal Analysis of TEFC Induction Motors, 2003 IAS Annual Meeting, 12 – 16 October 2003, Salt Lake City, USA.